View Article Online / Journal Homepage / Table of Contents for this issue
Dynamic Article Links

Dalton Transactions

Cite this: *Dalton Trans.*, 2012, **41**, 831

www.rsc.org/dalton

PAPER

Development of a borondipyrromethene-based Zn^{2+} fluorescent probe: solvent effects on modulation sensing ability†

Chunchang Zhao,* Yulin Zhang, Peng Feng and Jian Cao

Received 29th April 2011, Accepted 3rd October 2011
DOI: 10.1039/c1dt10797f

Published on 17 November 2011 on http://pubs.rsc.org | doi:10.1039/C1DT10797F
Downloaded by FORDHAM UNIVERSITY on 20 December 2012

A borondipyrromethene-based Zn^{2+} fluorescent probe **BODPAQ** was designed and synthesized. The chelators in **BODPAQ**, 2,2′-dipicolylamine (DPA) and 8-aminoquinoline (AQ), coordinate to Zn^{2+} in a synergic manner. As a result, **BODPAQ** displays high Zn^{2+} selectivity with a dramatic enhanced emission accompanied by a notable hypsochromic shift due to the binary inhibition effect of PET and ICT mechanisms, enabling the detection of Zn^{2+} by both ratiometric and normal turn-on fluorescence methods in acetonitrile. Interestingly, the sensitivity of **BODPAQ** towards Zn^{2+} changes upon varying the compositions of buffer solutions. In 3-morpholinopropanesulfonic acid (MOPS) buffer aqueous solution (50% CH_3CN), **BODPAQ** displays the highest sensitivity for Zn^{2+}, while in citrate–phosphate buffer, **BODPAQ** shows no response to Zn^{2+}.

Introduction

Fluorescent probes are expected to be powerful tools for the analysis of many biologically relevant heavy transition-metal ions because of the simplicity, high sensitivity and high spatial resolution of fluorescence.[1] Among heavy transition-metal ions, Zn^{2+} is an attractive target in the design of fluorescent probes due to the significant biological roles of zinc. Zinc plays vital roles in catalytic functions of proteins, gene expression, apoptosis, neurotransmission, and so forth.[2] It is also known that disorders of Zn^{2+} metabolism are associated with physical growth retardation and neurological diseases such as cerebral ischemia and Alzheimer's disease.[3] Therefore, measurement of Zn^{2+} is essential but challenging due to the biological significance and the interference of other metals in biological systems. High sensitivity and selectivity are essential properties that an ideal fluorescent probe for zinc should possess. Accordingly, there have been considerable efforts to develop fluorescent sensors for Zn^{2+}.[4] The most currently available small molecule fluorescent probes detect Zn^{2+} by an increase or decrease of the emission intensity,[5] derived mainly from aryl sulfonamides,[6] and bulk xanthenone fluorophores.[7,8] However, as the change in fluorescence intensity is the only detection signal, factors such as the probe concentration, instrumental efficiency, and environmental conditions can interfere with the signal output.[9] It is therefore desirable to eliminate the effects of these factors. Ratiometric sensors that exhibit a spectral shift upon binding to Zn^{2+} can eliminate most or all ambiguities by self-calibration of two emission bands. To date, only a few ratiometric probes for Zn^{2+} have been reported.[10]

Although a variety of fluorescent sensors for Zn^{2+} have been developed successfully, based on photo-induced electron transfer (PET) or intramolecular charge transfer (ICT) mechanisms, few fluorescent sensors with both PET and ICT sensing behaviors have been constructed. Given the successful application of PET or ICT in designing fluorescent probes,[5–10] we envisioned that combination of the two sensing behaviors could be exploited as an interesting platform for fluorescent Zn^{2+} probes. Here, we decided to employ a combination of the key features of ICT and PET in our ratiometric probe design. Based on this strategy, a new borondipyrromethene-based ratiometric probe **BODPAQ** with both PET and ICT sensing behaviors was reported. The probe was designed by combining two chelators, 2,2′-dipicolylamine (DPA) and 8-aminoquinoline (AQ), into one borondipyrromethene molecule. Given the successful application of DPA[7,8d,8e] and 8-aminoquinoline[7g,11] derivatives in Zn^{2+} sensing, we expected a combination of DPA and quinoline to be advantageous. These two receptors are expected to coordinate to metals in a synergic manner, thus improve the Zn^{2+} selectivity. The binding of Zn^{2+} to **BODPAQ** induced not only emission enhancement but also an emission shift due to the binary inhibition effect of PET and ICT mechanisms, enabling the detection of Zn^{2+} by both ratiometric and normal turn-on fluorescence methods. It is known that compositions of solutions affect the binding ability of fluorescent probes to analytes. Changing the solvent from organic to aqueous solutions, the response can be significantly affected by the compositions of buffer solutions and the emission response can completely vanish. The present study also demonstrates in detail how solvent effects modulate the binding affinity and selectivity of **BODPAQ** towards Zn^{2+}.

Key Laboratory for Advanced Materials and Institute of Fine Chemicals, East China University of Science & Technology, Shanghai, 200237, P. R. China. E-mail: zhaocchang@ecust.edu.cn; Tel: +86 6425 2388

† Electronic supplementary information (ESI) available: List of materials and general experimental methods; NMR spectra of the new compounds; Absorption and emission spectra of **BODPAQ** in aqueous solutions; Ratiometric calibration curve. See DOI: 10.1039/c1dt10797f

Published on 17 November 2011 on http://pubs.rsc.org | doi:10.1039/C1DT10797F
Downloaded by FORDHAM UNIVERSITY on 20 December 2012

Experimental

General information

All chemicals were purchased from commercial suppliers unless otherwise specified. Et_3N, chloroform and 1,2-dichloroethane were used as received without further purification. Anhydrous *N*,*N*-dimethylformamide (DMF) and toluene were dried and distilled immediately prior to use. 2-chloro-5-benzoyl-pyrrole[12] and 2,4-dimethyl-3-ethylpyrrole[12] were prepared according to literature procedures.

^{1}H NMR and ^{13}C NMR spectra were recorded on a spectrometer operating at 400 MHz and 100 MHz, respectively. Deuterated chloroform was used as the solvent and TMS as the internal standard. Mass spectra were measured on an HP 1100 LC-MS spectrometer. UV-vis spectra were measured using a Shimadzu UV-2550 spectrophotometer. Fluorescence spectroscopic measurements were conducted on a Varian Cary Eclipse fluorescence spectrophotometer.

For absorption or fluorescence measurements, compounds were dissolved in DMSO to obtain stock solutions (2–5 mM). These stock solutions were diluted with CH_3CN or aqueous solutions to the desired concentration.

Synthesis of 3-chloro-5,7-dimethyl-6-ethyl-8-phenyl-BODIPY (2). A mixture of 2-chloro-5-benzoyl-pyrrole (0.555 g, 2.71 mmol) and $POCl_3$ (0.75 mL) in 30 mL CH_2Cl_2 was stirred for 1 h at room temperature. To this reaction mixture was added 2,4-dimethyl-3-ethylpyrrole (1.000 g, 8.12 mmol) in CH_2Cl_2, and the mixture was further stirred for 36 h. The reaction mixture was slowly poured into saturated aqueous $NaHCO_3$ (50 mL) under ice-cold conditions, washed with water, dried over anhydrous Na_2SO_4, and evaporated *in vacuo*. The residue was dissolved in toluene before Et_3N (1 mL) was added and the mixture was stirred for 1 h at room temperature. $BF_3{\cdot}OEt_2$ (0.9 mL, 6.62 mmol) was added *via* syringe and the reaction was stirred at 100 °C for 6 h. After cooling, the reaction mixture was diluted with chloroform and washed with saturated aqueous $NaHCO_3$ solution and brine, dried over Na_2SO_4, and evaporated. The residue was purified by column chromatography (silica gel, 1 : 50 EtOAc/hexane) to give **2** (0.336 mg, 42%) as an orange crystalline solid. ^{1}H NMR ($CDCl_3$, 400 MHz): δ 7.55–7.47 (m, 3H), 7.35–7.30 (m, 2H), 6.24 (d, 1H), 6.21 (d, 1H), 2.63 (s, 3H), 2.36 (q, 2H), 1.43 (s, 3H), 1.04 (t, 3H); ^{13}C NMR (100 MHz, $CDCl_3$) δ 163.0, 142.0, 140.4, 136.7, 136.4, 136.3, 133.6, 133.5, 133.3, 129.4, 128.9, 128.5, 126.0, 114.9, 114.8, 17.13, 14.2, 13.3, 12.3; HRMS (ESI) calcd for $C_{19}H_{19}N_2BClF_2$: 359.1298. Found: 359.1285 $[M + H]^+$.

Synthesis of 3-(4-(bis(pyridine-2-ylmethyl)amino))-5,7-dimethyl-6-ethyl-8-phenyl-BODIPY (3). To a solution of **2** (0.62 g 1.73 mmol) in 30 mL CH_3CN was added DPA (0.62 g, 2.60 mmol) and Et_3N (5 mL), and the reaction mixture was refluxed for 12 h. Excess CH_3CN was removed under vacuum, and the residue was dissolved in ethyl acetate, washed with H_2O and dried over Na_2SO_4. The crude product was purified by flash chromatography (silica gel, eluent: hexane/EtOAc 3 : 1) to afford **3** (0.630 g, 69%). ^{1}H NMR (400 MHz, $CDCl_3$) δ 8.52 (s, 1H), 8.51 (s, 1H), 7.69–7.63 (m, 2H), 7.48 (s, 1H), 7.46 (s, 1H), 7.44–7.39 (m, 3H), 7.33–7.30 (m, 2H), 7.19–7.15 (m, 2H), 6.35 (d, 1H), 5.94 (d, 1H), 5.09 (s, 4H), 2.49 (s, 3H), 2.34 (q, 2H), 1.36 (s, 3H), 0.98 (t, 3H); ^{13}C NMR (100 MHz, $CDCl_3$) δ 161.4, 157.5, 147.60, 136.8, 135.5, 134.7, 133.7, 133.0, 132.3, 131.1, 129.7, 128.4, 128.0, 122.3, 121.8, 110.1, 58.2, 58.1, 17.2, 14.8, 12.3, 11.4; HRMS (ESI) calcd for $C_{31}H_{29}N_5BF_2$: 520.2484. Found: 520.2474 $[M - H]^-$.

Synthesis of 2-formyl-3-(4-(bis(pyridine-2-ylmethyl)amino))-5,7-dimethyl-6-ethyl-8-phenyl-BODIPY (4). A mixture of DMF (10 mL) and $POCl_3$ (10 mL) was stirred in an ice bath for 5 min under argon. After warming to room temperature, it was stirred for an additional 1 h. A solution of **3** (0.47 g, 0.90 mmol) in 10 mL chloroform was then added, and the resulting mixture was stirred for 2 h at room temperature. The reaction mixture was cooled to room temperature and slowly poured into saturated aqueous Na_2CO_3 (30 mL) under ice-cold conditions. After warming to room temperature, the reaction mixture was further stirred for 30 min and washed with water. The organic layers were dried over anhydrous Na_2SO_4, and evaporated *in vacuo*. The crude product was further purified using column chromatography (alumina gel, EtOAc/hexane = 1 : 3) to give **4** (0.45 g, 91%). ^{1}H NMR (400 MHz, $CDCl_3$) δ 9.67 (s, 1H), 8.53 (d, 2H), 7.73–7.67 (m, 2H), 7.58 (s, 1H), 7.56 (s, 1H), 7.52–7.46 (m, 3H), 7.36–7.33 (m, 2H), 7.21–7.16 (m, 2H), 6.73 (s, 1H), 4.88 (s, 4H), 2.67 (s, 3H), 2.38 (q, 2H), 1.45 (s, 3H), 1.03 (t, 3H); ^{13}C NMR (100 MHz, $CDCl_3$) δ 185.0, 157.8, 149.3, 140.9, 140.3, 136.7, 133.6, 131.6, 131.5, 129.4, 129.1, 128.5, 128.4, 124.0, 123.9, 122.8, 122.3, 59.3, 59.2, 17.2, 14.2, 13.4, 12.2; HRMS (ESI) calcd for $C_{32}H_{29}N_5OBF_2$: 548.2433. Found: 548.2457 $[M - H]^-$.

Synthesis of 2-(quinolin-8-ylaminomethyl)-3-(4-(bis(pyridine-2-ylmethyl)amino))-5,7-dimethyl-6-ethyl-8-phenyl-BODIPY (BODPAQ). To 20 mL 1,2-dichloroethane was added **4** (0.55 g, 1 mmol) and 8-aminoquinoline (0.15 mg, 1.03 mmol). The reaction was stirred for 24 h at room temperature. A portion (0.26 g, 1.23 mmol) of $NaB(OAc)_3H$ was then added and the reaction mixture was stirred overnight. The solvent was removed under vacuum, and the residue was purified by flash chromatography (alumina gel, eluent: hexane/EtOAc 5 : 1) to afford **BODPAQ** (0.170 g, 25%). ^{1}H NMR (400 MHz, $CDCl_3$) δ 8.65–8.62 (d, 1H), 8.49 (d, 2H), 8.06–8.02 (m, 1H), 7.70 (s, 1H), 7.68 (s, 1H), 7.64–7.58 (m, 2H), 7.41–7.27 (m, 7H), 7.10 (t, 2H), 7.04 (d, 1H), 6.53 (d, 1H), 6.39 (s, 1H), 4.85 (s, 4H), 4.14 (s, 2H), 2.62 (s, 3H), 2.36 (q, 2H), 1.38 (s, 3H), 1.01 (t, 3H); ^{13}C NMR (100 MHz, $CDCl_3$) δ 159.1, 158.5, 154.0, 149.1, 146.7, 144.5, 138.2, 137.9, 137.1, 136.7, 135.9, 134.7, 133.2, 131.4, 130.6, 130.4, 129.4, 128.7, 128.5, 128.10, 127.7, 124.3, 122.9, 122.1, 121.2, 114.3, 105.7, 58.6, 41.0, 17.2, 14.6, 12.8, 11.8; HRMS (ESI) calcd for $C_{41}H_{39}N_7BF_2$: 678.3328. Found: 678.3338 $[M + H]^+$.

Results and discussion

Synthesis

The designed probe **BODPAQ** was synthesized in 5 steps as shown in Scheme 1. DPA was firstly introduced into the BODIPY core by S_N2 nucleophilic substitution. Subsequent formylation of the 2-position of the BODIPY core was achieved by Vilsmeier–Haack reactions using DMF/$POCl_3$ in chloroform.[13] Condensation of 1 equiv of 8-aminoquinoline with monoaldehyde **4** in 1,2-dichloroethane gave essentially pure intermediate imine, and

 This journal is © The Royal Society of Chemistry 2012

Published on 17 November 2011 on http://pubs.rsc.org | doi:10.1039/C1DT10797F
Downloaded by FORDHAM UNIVERSITY on 20 December 2012

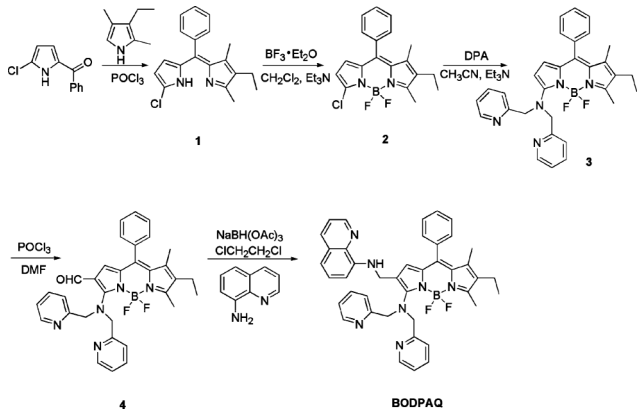

Scheme 1 Synthesis of **BODPAQ**.

reduction of the imine under mild conditions using $NaBH(OAc)_3$ in DCE gave **BODPAQ** in 25% yield.[7g,14]

Spectroscopic properties of BODPAQ and its pH dependence

The spectroscopic evaluation of **BODPAQ** was firstly performed in organic solvents of varying polarity. The optical features are characteristics of the BODIPY platform. As is evident from Table 1, **BODPAQ** shows almost identical absorption and fluorescence spectra in the various solvents.[15] The main S_0–S_1 absorption transition band, centered between 553 and 563 nm in the pure solvents, shows minor solvent-dependent variation and the maximum shifts of the absorbance are only 10 nm. Similar to the absorption spectra, the emission spectra also show minor solvent-dependent shifts. The maximum emission wavelength of **BODPAQ** is in the 578–587 nm range and the emission shows low fluorescence quantum yield (<0.03), especially in acetonitrile and methanol, where the fluorescence quantum yield is lower than 0.007.

The spectroscopic characteristics of **BODPAQ** were then evaluated in a series of aqueous solutions with varying acetonitrile content (Fig. S1, ESI†). **BODPAQ** exhibits a strong absorption band in the visible region centered at 560 nm in acetonitrile, and the maximum undergoes a slightly blue-shift from 560 nm to 552 nm with decreasing concentrations of CH_3CN in aqueous solutions from 100% to 10%. Emission spectral changes caused by the concentration of acetonitrile are in good agreement with the hypsochromic shift in the absorption spectra. Upon excitation at 560 nm, an emission spectrum with a maximum at 581 nm was observed in CH_3CN, and the emission band is finally shifted to 562 nm when excited at 552 nm in aqueous solution (10 mM Tris-HCl, 10% CH_3CN, 0.1 M KNO_3).

Table 1 Spectroscopic data for **BODPAQ** in various solvents

Solvent	λ_{abs} (nm)	λ_{em} (nm)	Φ_F
Methanol	553	575	0.005
Acetonitrile	560	581	0.007
Acetone	558	582	0.015
DMSO	562	587	0.013
Dichloromethane	559	586	0.019
Benzene	563	587	0.027
Hexane	560	582	0.022

The pH effect on the fluorescence spectra was investigated in acetonitrile/water (50 : 50, v/v) solution (Fig. 1). The fluorescence spectrum of **BODPAQ** exhibits an emission band with a maximum at 579 nm, a small (2 nm) blue shift compared to that in CH_3CN. The emission intensity at 579 nm displays little change between pH 6 and 10. However, a distinct emission hypsochromic shift from 579 nm to 560 nm can be observed when increasing the acidity from pH 6 to 5. This phenomenon could be attributed to the protonation of the tertiary amine in DPA, which inhibits the ICT interaction and results in a blue-shift in emission. Further increasing the acidity from pH 5 to 3, a dramatic emission enhancement occurs due to the reduced PET process by protonation of the aromatic amine in AQ. A similar protonation process has been observed in the DPA-based sensors.[9d,10c] The process was further studied in detail by ^1H NMR titration experiments of **BODPAQ** with HCl in CD_3CN (Fig. 2). As shown in Fig. 2, protonation with 1 equiv. HCl triggers a clear downfield shift up to $\Delta\delta = 0.31$ ppm for Ha. The chemical shift of Hc, in the *ortho* position of the pyridine ring, also underwent a downfield shift from 8.54 to 8.60 ppm. These results hint that the proton should firstly bind to the nitrogen on the DPA group. Notably, upon increasing HCl to more than 5 equiv., the chemical shift of Hd′, adjacent to the amino group in quinoline, moved from 6.52 to 7.13 ppm ($\Delta\delta = 0.61$ ppm), which clearly confirms the protonation of the aromatic amine in AQ.

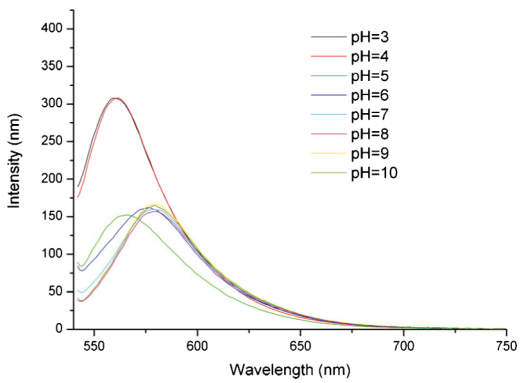

Fig. 1 Effect of pH on the fluorescence of **BODPAQ** (5 μM) in acetonitrile/water (50 : 50, v/v) solution, excitation wavelength: 530 nm.

Spectroscopic response of BODPAQ to Zn^{2+} in organic solvents

The spectra of **BODPAQ** are stable at around pH 7.0, so the titration experiments of **BODPAQ** with Zn^{2+} were carried out at pH 7.4. In acetonitrile (Fig. 3 and Fig. S2, ESI†), upon gradual addition of Zn^{2+}, a decrease in the absorption band at 560 nm and a concomitant increase of a new band at 520 nm were observed with a distinct isosbestic point at 530 nm; at the same time the color of the solution turned from purple to light pink. A significant blue shift of 40 nm of the absorption wavelength implies the coordination of the tertiary amino group in DPA to Zn^{2+}, which decreases the electron-donating ability of the tertiary amino group and leads to a blue-shift in absorption.[9d] The absorption bands at 560 nm and 520 nm change linearly up to a 1 : 1 ratio (Zn^{2+}/**BODPAQ**), which is consistent with the formation of a 1 : 1 complex. The K_d of a 1 : 1 Zn^{2+}/**BODPAQ** complex was determined to be 1.81×10^5 using Benesi–Hildebrand plots (see ESI†).

Published on 17 November 2011 on http://pubs.rsc.org | doi:10.1039/C1DT10797F
Downloaded by FORDHAM UNIVERSITY on 20 December 2012

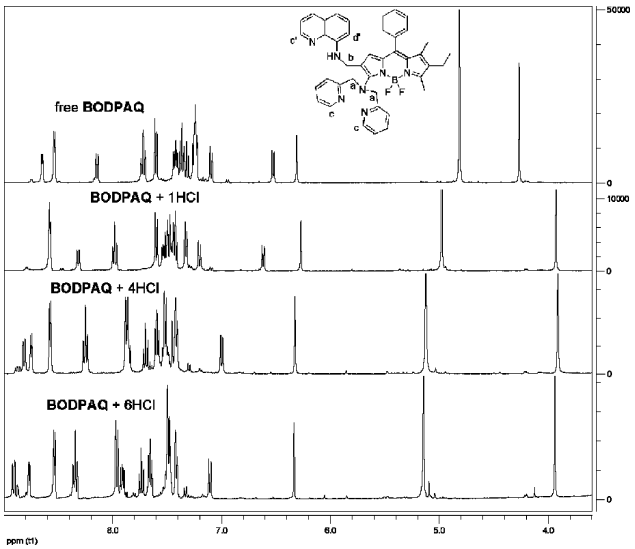

Fig. 2 Part of the ^{1}H NMR spectra of **BODPAQ** and **BODPAQ** + HCl (1, 4, 6 equiv.) in CD_3CN.

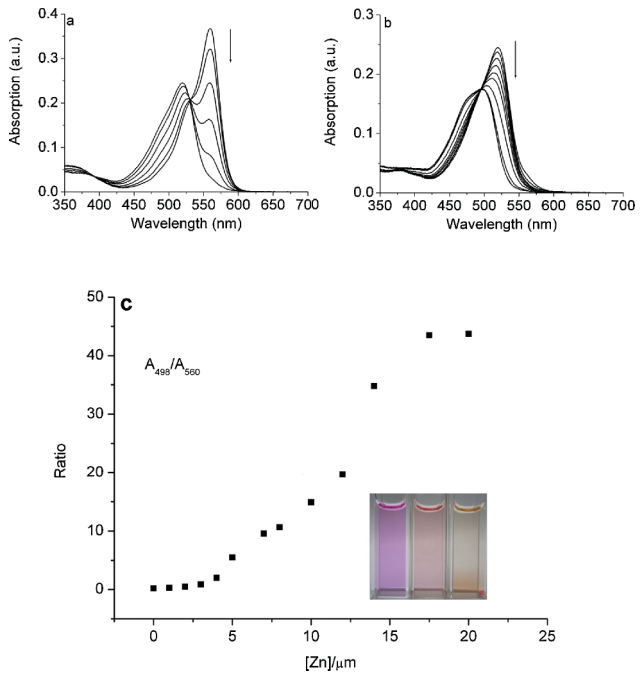

Fig. 3 (a) Absorption spectra of **BODPAQ** (5 μM) upon addition of Zn^{2+} at 0, 0.2, 0.4, 0.6, 0.8, 1.0 equiv. with respect to **BODPAQ** in CH_3CN. (b) Absorption spectra of **BODPAQ** (5 μM) upon addition of Zn^{2+} at 1.0, 1.2, 1.4, 1.6, 1.8, 2.0, 2.4, 2.8, 3.5, 4.0 equiv. with respect to **BODPAQ** in CH_3CN. (c) Ratio of absorbance at 498 nm and absorbance at 560 nm as a function of Zn^{2+} concentration. Inset: Color of solutions of **BODPAQ** in the presence of Zn^{2+} (right: **BODPAQ**, middle: **BODPAQ**+Zn^{2+} (1 equiv.), left: **BODPAQ**+Zn^{2+} (4 equiv.).

With higher [Zn^{2+}] (1–4 equiv.), a significant decrease at 520 nm was observed accompanied by the hypsochromic shift to 498 nm. These results can be explained in terms of the strength of the interaction between Zn^{2+} and the tertiary amino group in DPA. Higher [Zn^{2+}], greater than 1 equiv., causes stronger interaction and leads to a further blue-shift in the spectra, suggesting another type of complex other than the 1 : 1 type is formed. The λ_{max} of the newly formed complex is blue-shifted by 60 nm and is responsible for the change in color from purple to light orange. This color change can be used for a "naked-eye" detection of Zn^{2+} in acetonitrile (Fig. 2c). Moreover, the ratios of the absorbance at 498 and 560 nm showed sigmoidal dependence on the [Zn^{2+}] concentration, with a 227-fold ratiometric enhancement (Fig. 2b). This indicates the capability of **BODPAQ** for detecting [Zn^{2+}] by absorption ratiometry.

In the fluorescence spectra (Fig. 4), free **BODPAQ** exhibits fluorescence with a maximum at 581 nm and quantum yield of 0.007, which is lower than that of compound **3** (0.02) because of the PET quenching from the AQ amino group. Upon addition of Zn^{2+} from 0 to 1 equiv., the λ_{max}^{em} undergoes a blue shift to 549 nm accompanied by a remarkable fluorescence enhancement (quantum yield 0.04), indicating that a inhibited PET and ICT process occurred with consequent ratiometric and turn-on fluorescence signals although both Φ_{free} and Φ_{Zn} are not high. Both the emission intensity at 549 nm and the intensity ratio, R (F_{549}/F_{581}, Fig. S3, ESI†), increase upon gradual addition of Zn^{2+}, which allows the detection of Zn^{2+} by both ratiometric and normal turn-on fluorescence methods. Continuous addition of Zn^{2+} from 1 to 4 equiv. leads to further dramatic enhancement of the emission intensity, and the fluorescence turns out to be stable when 4 equiv. Zn^{2+} was added; higher [Zn^{2+}] does not lead to any change. As [Zn^{2+}] increases from 1 to 4 equiv., the emission wavelength is also hypsochromically shifted from 549 nm to 535 nm, resulting from the stronger interaction of Zn^{2+} with the tertiary amino group in

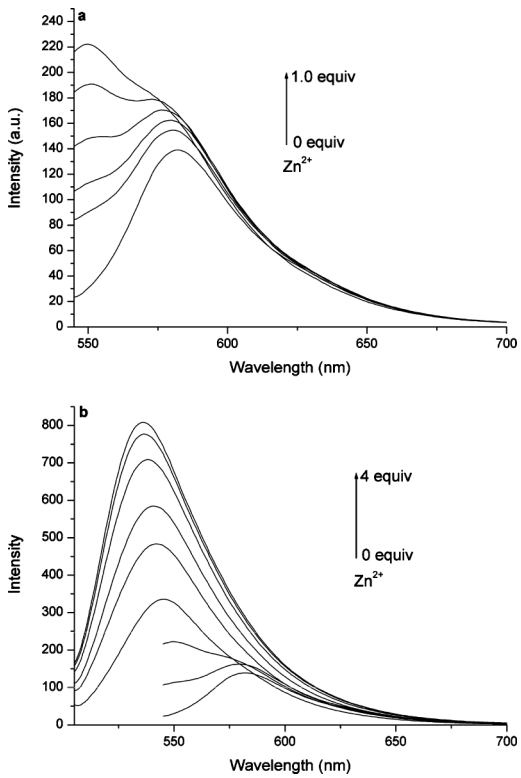

Fig. 4 (a) Emission spectra of **BODPAQ** (5 μM) upon addition of Zn^{2+} (0, 0.2, 0.4, 0.6, 0.8, 1.0 equiv. with respect to **BODPAQ**) in CH_3CN; (b) Emission spectra of **BODPAQ** (5 μM) upon addition of Zn^{2+} (0, 0.4, 1.0, 1.2, 1.6, 2.6, 3.2, 3.6, 4.0 equiv. with respect to **BODPAQ**) in CH_3CN. Excitation wavelength: 530 nm.

This journal is © The Royal Society of Chemistry 2012

Published on 17 November 2011 on http://pubs.rsc.org | doi:10.1039/C1DT10797F
Downloaded by FORDHAM UNIVERSITY on 20 December 2012

the newly formed complex other than the 1 : 1 complex. It is worth noting that the newly formed complex is highly fluorescent with quantum yield around 0.20, which makes **BODPAQ** a promising turn-on fluorescent probe for [Zn^{2+}].

Other organic solvents were also used to study the binding properties of **BODPAQ** with Zn^{2+}. **BODPAQ** responds to Zn^{2+} in the same way in methanol or ethanol as it does in CH_3CN (Fig. S4–S5, ESI†). Upon titration with Zn^{2+}, the absorption spectra show the evident hypsochromic shift from 552 nm to 514 nm with [Zn^{2+}] up to 1 equiv. More [Zn^{2+}] also induced the new absorption band at 514 nm to shift to 505 nm, but the shift is less pronounced. With increasing [Zn^{2+}], the $\lambda_{max}{}^{em}$ also undergoes a blue shift from 575 nm to 544 nm, accompanied by a significant fluorescence enhancement (quantum yield changes from 0.005 to 0.1).

The possible 1 : 1 binding model of Zn^{2+} and **BODPAQ** in acetonitrile therefore can be deduced and is shown in Scheme 2, which is further confirmed by mass spectrometry. The ESI mass spectrum of Zn^{2+} (1 equiv.) + **BODPAQ** has a major peak with m/z of 840.2211 ([Zn^{2+} + **BODPAQ** + ClO_4^-]$^+$), which corresponds to a 1 : 1 complex (Fig. S6, ESI†).

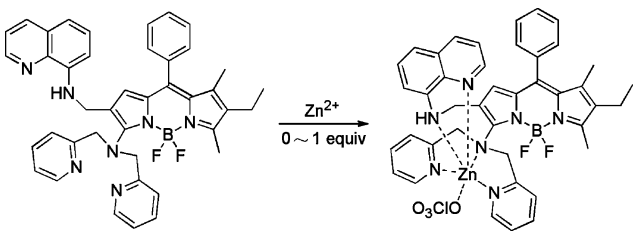

Scheme 2 Proposed binding model of Zn^{2+} with **BODPAQ**.

To validate the nature of the interaction of **BODPAQ** and Zn^{2+}, ^{1}H NMR titrations in CD_3CN were carried out, as shown in Fig. 5. Upon addition of 1 equiv. Zn^{2+}, all the protons of DPA and AQ experience significant changes. The coordination triggers a clear change of protons Ha and Hb from two singlet signals to six doublet signals, indicating that the nitrogen atom attached to the methylene group strongly bonds with Zn^{2+}. Protons of pyridines show downfield or upfield shifts as a result of the *N*-metal coordination effect, such as Hc at the *ortho* position, one from 8.54 to 9.15, and another from 8.54 to 8.45. Meanwhile, similar shifts are also observed for the protons of quinoline, suggesting the direct interaction between the quinoline platform and metal ions. More Zn^{2+} does not lead to any evident change in the ^{1}H NMR spectrum. All these results indicate a 1 : 1 binding model between **BODPAQ** and Zn^{2+}. Unfortunately, we cannot give direct evidence by mass and ^{1}H NMR spectra to explain the phenomenon that a new type of complex other than a 1 : 1 complex is formed by introducing more than 1 equiv. Zn^{2+}, as observed by UV-vis and fluorescence spectra.

The coordination of **BODPAQ** to Zn^{2+} was also explored by molecular modeling. The conformation of the Zn^{2+}/**BODPAQ** complex was optimized by density functional theory (DFT) calculations at the B3LYP/6-311G level (Gaussian 2009).[16] As shown in Fig. 6, the zinc ion in Zn^{2+}/**BODPAQ** is coordinated by the three nitrogen atoms of one DPA arm, two N atoms of aminoquinoline, and a solvent molecule or a ClO_4^- anion to form the distorted six-coordination geometry. The theoretical study shows that the amines both in DPA and AQ are directly

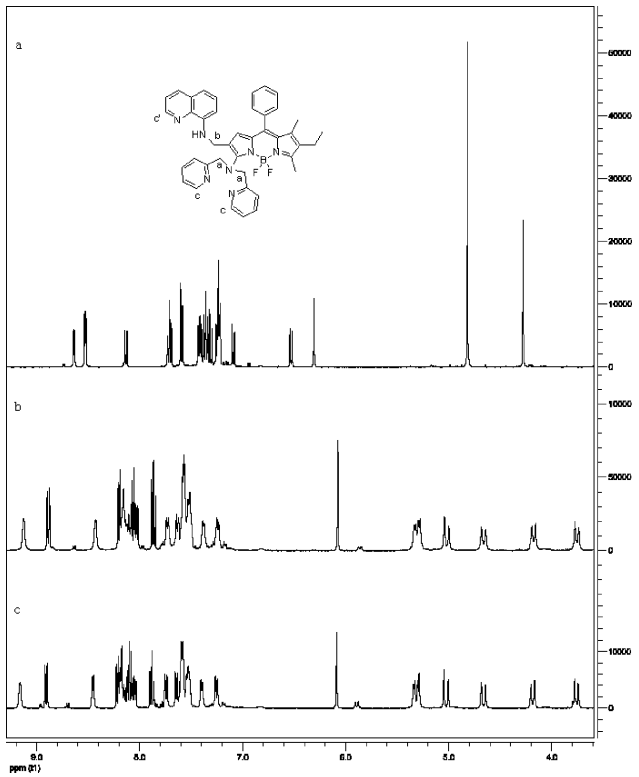

Fig. 5 Part of the ^{1}H NMR spectra of **BODPAQ** in CD_3CN in the absence and presence of Zn^{2+}. (a) free **BODPAQ**; (b) **BODPAQ** + 1 equiv. Zn^{2+}; (c) **BODPAQ** + 4 equiv. Zn^{2+}.

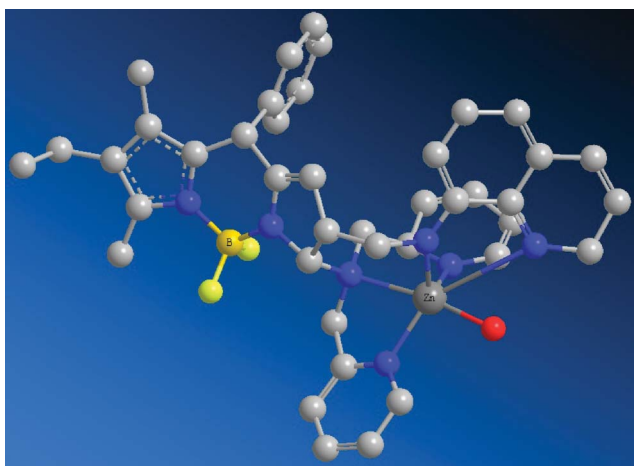

Fig. 6 Structure of Zn^{2+}/**BODPAQ** complex estimated by density functional theory calculations. Hydrogen atoms, tetrahedral perchlorate and solvent molecules are omitted for clarity.

coordinated to Zn^{2+}, thus the dipole moment is distinctly changed in the Zn^{2+} binding process, therefore the PET and ICT process from coordination atoms to the fluorophore is blocked.

The selectivity of fluorescence response of **BODPAQ** to metal ions was then investigated by titration of different ions in CH_3CN. As illustrated in Fig. 7, only Zn^{2+} and Cd^{2+} enhance the emission of **BODPAQ** accompanied by a notable hypsochromic shift. Alkali and alkaline earth metal ions such as Ca^{2+}, Mg^{2+}, Na^+, and K^+ do not induce any emission change. Most heavy transition metal ions such as Fe^{2+}, Hg^{2+}, and Mn^{2+} have little influence

Downloaded by FORDHAM UNIVERSITY on 20 December 2012
Published on 17 November 2011 on http://pubs.rsc.org | doi:10.1039/C1DT10797F

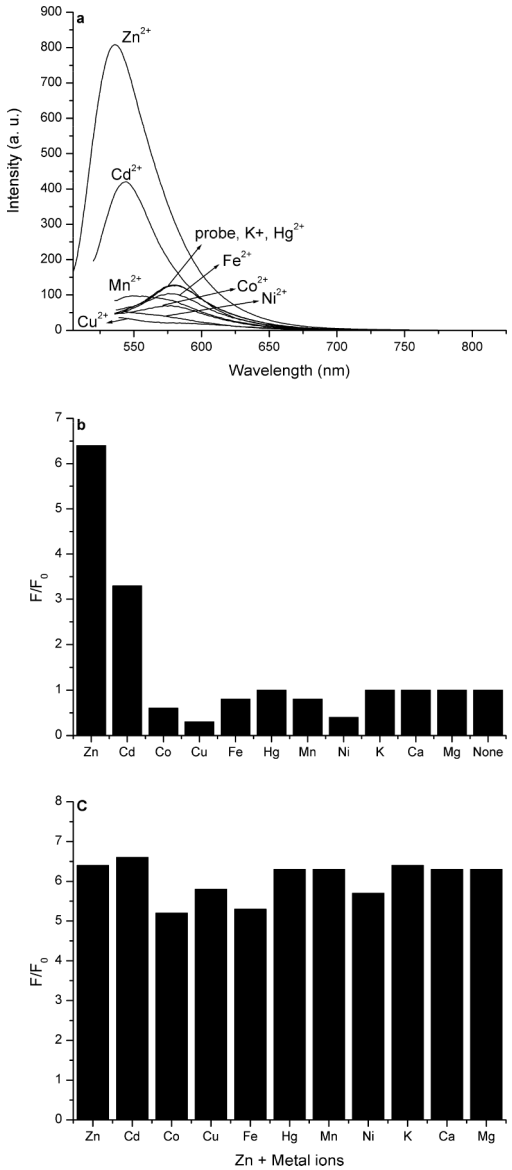

Fig. 7 (a) Fluorescence spectra of **BODPAQ** (5 μM) in the presence of various metal ions (4 equiv. of Zn^{2+}, Cd^{2+}, Co^{2+}, Cu^{2+}, Fe^{2+}, Hg^{2+}, Mn^{2+}, and Ni^{2+} and 100 equiv. of K^+, Ca^{2+}, and Mg^{2+}) in CH_3CN. (b) Histogram of F/F_0 induced by various metal ions. (c) The ratio fluorescence response (F_{535}/F_0) of **BODPAQ** (5 μM) containing 4 equiv. Zn^{2+} to the selected metal ions.

on the fluorescence intensity of **BODPAQ** while Cu^{2+}, Co^{2+} and Ni^{2+} decrease the emission intensity. Therefore, **BODPAQ** shows distinct selectivity for Zn^{2+} over other cations except for Cd^{2+}.

To further check the Zn^{2+}-specific amplified fluorescence change of **BODPAQ**, titration experiments of **BODPAQ**-Zn^{2+} complex (1 : 4) were conducted by the addition of 100 equiv. of Ca^{2+}, Mg^{2+}, Na^+, K^+ and 4 equiv. of Fe^{2+}, Hg^{2+}, and Mn^{2+} Cu^{2+}, Co^{2+}, Ni^{2+}. The experimental results indicate that the emission profile of the **BODPAQ**-Zn^{2+} complex is not influenced by these metal ions, indicating the high affinity and selectivity for Zn^{2+}.

The influence of solvent systems on Zn^{2+} binding affinity and selectivity

The binding properties of **BODPAQ** with Zn^{2+} obtained from the studies in pure acetonitrile do not necessarily correspond to those that apply in aqueous solutions. Therefore, the influence of the solvent systems on the binding property and selectivity was studied in different buffer solutions.

The binding property and selectivity were firstly investigated in 3-morpholinopropanesulfonic acid (MOPS) buffer aqueous solution (50 mM, 50% CH_3CN, pH = 7.3). Compared to the spectral response of **BODPAQ** to Zn^{2+} in 100% acetonitrile, the measured absorption spectra of free **BODPAQ** exhibits a strong absorption band centered at 557 nm in MOPS buffer aqueous solution with the λ_{max} undergoing a slight blue-shift (Fig. 8a). When Zn^{2+} was added, a distinct decrease of the absorption band at 557 nm can be observed accompanied by a hypsochromic shift to 511 nm with a distinct isobestic point at 520 nm, which is consistent with the presence of only two species, free ligand and Zn^{2+}-ligand complex. The titration profile shows the absorption at 557 nm descends almost linearly until a ligand-to-metal ratio of 1 : 1 is reached. Further addition of Zn^{2+} does not affect the absorption spectrum, suggesting a 1 : 1 stoichiometry for the zinc

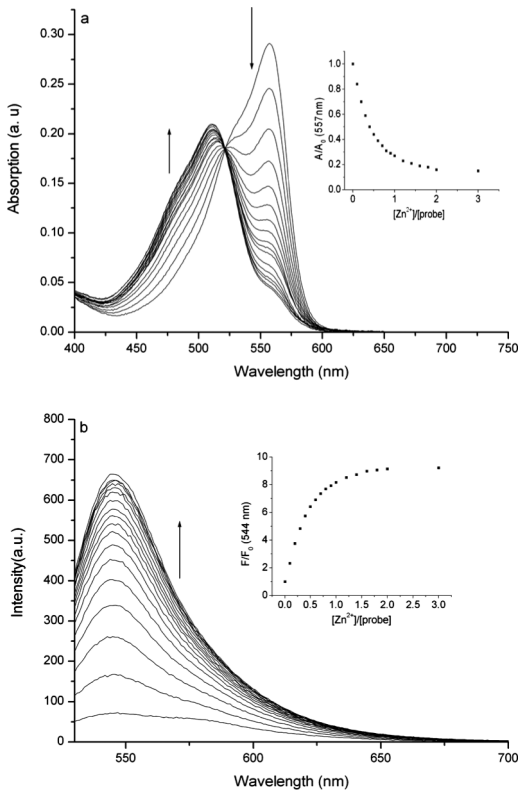

Fig. 8 (a) Absorption spectra of **BODPAQ** (5 μM) upon addition of Zn^{2+} (0, 0.1, 0.2, 0.3, 0.4, 0.5, 0.6, 0.7, 0.8, 0.9, 1.0, 1.2, 1.4, 1.6, 1.8, 2.0, 3.0 equiv. with respect to **BODPAQ** in CH_3CN/buffer (50 : 50); Inset is the titration profile according to the absorbance at 557 nm. (b) Emission spectra of **BODPAQ** (5 μm) upon addition of Zn^{2+} (0, 0.1, 0.2, 0.3, 0.4, 0.5, 0.6, 0.7, 0.8, 0.9, 1.0, 1.2, 1.4, 1.6, 1.8, 2.0, 3.0 equiv. with respect to **BODPAQ** in CH_3CN/buffer (50 : 50), Inset is the titration profile according to F/F_0, the fluorescence intensity ratio at 544 nm.

 This journal is © The Royal Society of Chemistry 2012

Published on 17 November 2011 on http://pubs.rsc.org | doi:10.1039/C1DT10797F
Downloaded by FORDHAM UNIVERSITY on 20 December 2012

complex. The binding constant was determined to be 0.94×10^5 using Benesi–Hildebrand plots (see ESI†).

Fluorescence titration of **BODPAQ** by Zn^{2+} in CH_3CN/MOPS buffer (50 : 50) aqueous solution exhibits a distinct emission enhancement (Φ_{free} = 0.005, Φ_{Zn} = 0.20) with the concentration of Zn^{2+} up to a molar ratio of 1 : 1, which is confirmed by Job's plot (Fig. 8b). An enhancement factor of 9 was observed. Higher concentrations of Zn^{2+} do not lead to noticeable fluorescence changes, suggesting that only a 1 : 1 Zn^{2+}-**BODPAQ** complex formed. The same as in acetonitrile, the Zn^{2+}-induced emission enhancement is caused by the PET blocking effect and inhibited ICT induced by the Zn^{2+} coordination to the AQ amino and tertiary amino groups in DPA. In addition, **BODPAQ** responds to metal ions in the same way as in methanol aqueous solutions (50 mM MOPS, 50% Methanol, pH 7.3) (Fig. S9, ESI†).

The fluorescence response of **BODPAQ** to various cations and its selectivity for Zn^{2+} were also examined in CH_3CN/MOPS buffer (50 : 50) aqueous solution (Fig. 9). Fluorescence enhancement of **BODPAQ** was not observed upon addition of 100 equiv. of alkali and alkaline earth metals including Na^+, K^+, Mg^{2+}, and Ca^{2+}. As for heavy transition metal ions, Fe^{2+}, Hg^{2+}, Mn^{2+}, and Pb^{2+} have little influence on the fluorescence intensity of **BODPAQ** while Cu^{2+}, Co^{2+} and Ni^{2+} obviously quench the fluorescence to some extent. Only when Zn^{2+} and Cd^{2+} were added was a remarkable fluorescence change detected. Note that Zn^{2+} induced much stronger enhancement of the fluorescence than Cd^{2+}. The competition experiments were then investigated by addition of various metal ions to the solution of **BODPAQ**-Zn^{2+} complex (1 : 4). Other metal ions promote no significant variation in the fluorescence intensity ratio (F/F_0) of the **BODPAQ**-Zn^{2+} complex, although Cu^{2+}, Ni^{2+} and Co^{2+} slightly quench the fluorescence and Cd^{2+} induces a slight fluorescence enhancement. These results suggest that **BODPAQ** has good selectivity for Zn^{2+} under the experimental conditions.

The fluorescence titration experiments were also carried out in other types of buffer solutions (HEPES, Tris-HCl, citrate–phosphate). As shown in Fig. 10, Zn^{2+} induced the highest ratio of F/F_0 in MOPS buffer solution. In other words, the highest fluorescence off/on ratio can be obtained and thus the highest sensitivity can be achieved in MOPS. When the buffer solutions were switched to HEPES (50 mM, 100 M KNO_3, 50% CH_3CN), Tris-HCl (10 mM Tris-HCl, 50% CH_3CN, 0.1 M KNO_3), and citrate–phosphate, the fluorescence ratio decreases and finally no response of **BODPAQ** to Zn^{2+} occurred in citrate–phosphate buffer. The sensitivity of **BODPAQ** to Zn^{2+} in different buffer solutions may indicate that the different environment around **BODPAQ** and different ionic strength could affect the binding affinity of the probe to metal ions.[17]

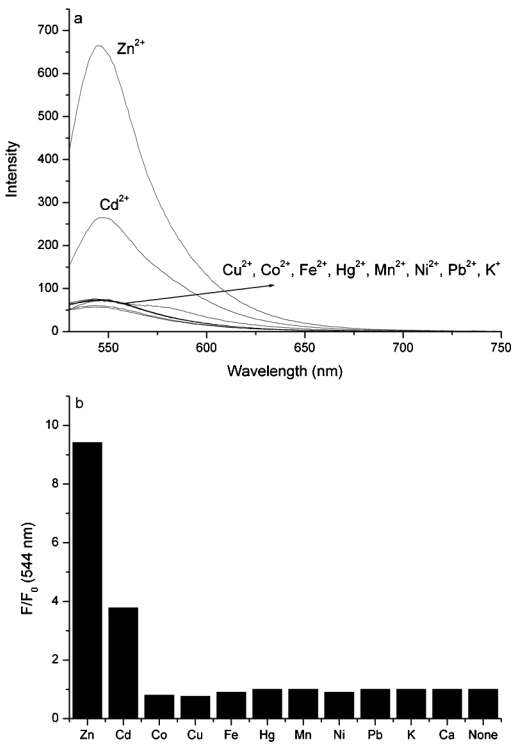

Fig. 9 (a) Fluorescence spectra of **BODPAQ** in the presence of various metal ions (4 equiv. of Zn^{2+}, Cd^{2+}, Co^{2+}, Cu^{2+}, Fe^{2+}, Hg^{2+}, Mn^{2+}, and Ni^{2+} and 100 equiv. of K^+, Ca^{2+}, and Mg^{2+}) in CH_3CN/MOPS buffer (50 : 50); (b) Histogram of F/F_0 (544 nm) induced by 4 equiv. of various metal ions.

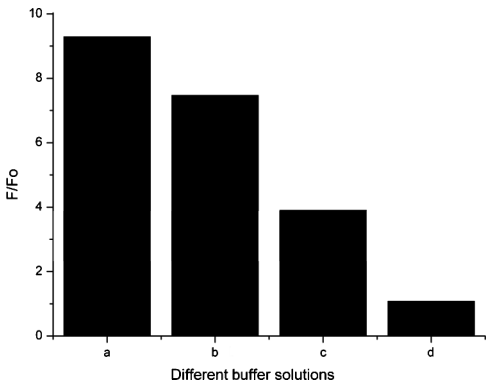

Fig. 10 Fluorescence intensity ratio of **BODPAQ** towards Zn^{2+} in different buffer solutions containing 50% CH_3CN as cosolvent, (a) F/F_0 is the fluorescence intensity ratio at 544 nm in MOPS buffer solution, (b) F/F_0 at 542 nm in HEPES buffer solution, (c) F/F_0 at 547 nm in Tris-HCl buffer solution, (d) F/F_0 at 577 nm in citrate–phosphate buffer solution.

Conclusion

A new borondipyrromethene-based fluorescent probe **BODPAQ** with both PET and ICT sensing behaviors has been synthesized. In this probe, two chelators, 2,2′-dipicolylamine (DPA) and 8-aminoquinoline (AQ), are combined into one borondipyrromethene molecule, which was designed to optimize the coordination to metals of the two chelators in a synergic manner, thus improve the Zn^{2+} selectivity. The interaction between the DPA group and Zn^{2+} inhibits the electron-donating ability of the amino group, and the interaction between the 8-AQ group and Zn^{2+} blocks the PET process. Therefore, the binding of Zn^{2+} to **BODPAQ** induced not only emission enhancement but also an emission shift due to the binary inhibition effect of the PET and ICT mechanisms. In acetonitrile, **BODPAQ** displays distinct fluorescence selectivity for Zn^{2+} with a dramatic enhanced emission accompanied by a notable hypsochromic shift among competing metal ions, although Cd^{2+} also induces an emission enhancement. More interestingly, **BODPAQ** displays the highest sensitivity for Zn^{2+} in MOPS among several buffer

Published on 17 November 2011 on http://pubs.rsc.org | doi:10.1039/C1DT10797F
Downloaded by FORDHAM UNIVERSITY on 20 December 2012

solutions used in this study. When the buffer solutions were then switched to HEPES, Tris-HCl, or citrate–phosphate respectively, the fluorescence sensitivity begins to decrease, and finally no response of **BODPAQ** to Zn^{2+} occurred in citrate–phosphate buffer. It should be noted that Zn^{2+} induced much stronger enhancement of the fluorescence than Cd^{2+}, however, it is still hard to distinguish successfully between Zn^{2+} and Cd^{2+} in aqueous solutions. To improve the Zn^{2+} specific amplified fluorescence in aqueous solutions, chelators with high affinity for Zn^{2+} should be introduced into the borondipyrromethene core. Strategies including introduction of *N*,*N*,*N*′-tri(pyridine-2-ylmethyl)ethane-1,2-diamine (TPEA)[5h,9d,18] instead of DPA are in progress.

Acknowledgements

We gratefully acknowledge the financial support by the National Science Foundation of China (grant no.: 20902021), the Scientific Research Foundation for the Returned Overseas Chinese Scholars (State Education Ministry), Key Laboratory of Photochemical Conversion and Optoelectronic Materials (TIPC, CAS) and the East China University of Science and Technology research funds. We also gratefully acknowledge Prof. Fu Wei for help in optimizing the Zn^{2+}/**BODPAQ** complex by density functional theory calculations.

Notes and references

1 (*a*) A. P. de Silva, H. Q. N. Gunaratne, T. Gunnlaugsson, A. J. M. Huxley, C. P. McCoy, J. T. Rademacher and T. E. Rice, *Chem. Rev.*, 1997, **97**, 1515–1566; (*b*) B. Valeur, *Molecular Fluorescence: Principles and Applications*; Wiley-VCH: Weinheim, NY, 2002.

2 (*a*) J. M. Berg and Y. Shi, *Science*, 1996, **271**, 1081–1085; (*b*) A. C. Burdette and S. J. Lippard, *Proc. Natl. Acad. Sci. U. S. A.*, 2003, **100**, 3605–3610; (*c*) B. L. Vallee and K. H. Falchuk, *Psychol. Rep.*, 1993, **73**, 79–118.

3 (*a*) D. W. Choi and J. Y. Koh, *Annu. Rev. Neurosci.*, 1998, **21**, 347–375; (*b*) J. H. Weiss, S. L. Sensi and J. K. Koh, *Trends Pharmacol. Sci.*, 2000, **21**, 395–401; (*c*) J. Y. Koh, S. W. Suh, B. J. Gwag, Y. Y. He, C. Y. Hsu and D. W. Choi, *Science*, 1996, **272**, 1013–1016.

4 Recent reviews for zinc sensors: (*a*) E. L. Que, D. W. Domaille and C. J. Chang, *Chem. Rev.*, 2008, **108**, 1517–1549; (*b*) E. M. Nolan and S. J. Lippard, *Acc. Chem. Res.*, 2009, **42**, 193–203; (*c*) Z. Dai and J. W. Canary, *New J. Chem.*, 2007, **31**, 1708–1718; (*d*) P. Jiang and J. Guo, *Coord. Chem. Rev.*, 2004, **248**, 205–229; (*e*) P. Carol, S. Sreejith and A. Ajayaghosh, *Chem.–Asian J.*, 2007, **2**, 338–348; (*f*) N. C. Lim, H. C. Freake and C. Brückner, *Chem.–Eur. J.*, 2005, **11**, 38–49; (*g*) D. W. Domaille, E. L. Que and C. J. Chang, *Nat. Chem. Biol.*, 2008, **4**, 168–175.

5 (*a*) T. W. Kim, J. Park and J.-I. Hong, *J. Chem. Soc., Perkin Trans. 2*, 2002, 923–927; (*b*) K. R. Gee, Z.-L. Zhou, W.-J. Qian and R. Kennedy, *J. Am. Chem. Soc.*, 2002, **124**, 776–778; (*c*) N. C. Lim, L. Yao, H. C. Freake and C. Brückner, *Bioorg. Med. Chem. Lett.*, 2003, **13**, 2251–2254; (*d*) T. Koike, T. Watanabe, S. Aoki, E. Kimura and M. Shiro, *J. Am. Chem. Soc.*, 1996, **118**, 12696–12703; (*e*) S. Aoki, S. Kaido, H. Fujioka and E. Kimura, *Inorg. Chem.*, 2003, **42**, 1023–1030; (*f*) T. Hirano, K. Kikuchi, Y. Urano, T. Higuchi and T. Nagano, *Angew. Chem., Int. Ed.*, 2000, **39**, 1052–1054; (*g*) A. Czarnik, *Acc. Chem. Res.*, 1994, **27**, 302–308; (*h*) K. Hanaoka, Y. Muramatsu, Y. Urano, T. Terai and T. Nagano, *Chem.–Eur. J.*, 2010, **16**, 568–572; (*i*) Z. Li, M. Yu, L. Zhang, M. Yu, J. Liu, L. Wei and H. Zhang, *Chem. Commun.*, 2010, **46**, 7169–7171; (*j*) X. Peng, X. Tang, W. Qin, W. Dou, Y. Guo, J. Zheng, W. Liu and D. Wang, *Dalton Trans.*, 2011, **40**, 5271–5277.

6 (*a*) C. J. Frederickson, E. J. Kasarskis, D. Ringo and R. E. Frederickson, *J. Neurosci. Methods*, 1987, **20**, 91–103; (*b*) M. C. Kimber, I. B. Mahadevan, S. F. Lincoln, A. D. Ward and E. R. T. Tiekink, *J. Org. Chem.*, 2000, **65**, 8204–8209; (*c*) C. J. Fahrni and T. V. O'Halloran, *J. Am. Chem. Soc.*, 1999, **121**, 11448–11458; (*d*) P. D. Zalewski, I. J. Forbes, R. F. Seamark, R. Borlinghaus, W. H. Betts, S. F. Lincoln and A. D. Ward, *Chem. Biol.*, 1993, **1**, 153–161.

7 (*a*) S. C. Burdette, G. K. Walkup, B. Spingler, R. Y. Tsien and S. J. Lippard, *J. Am. Chem. Soc.*, 2001, **123**, 7831–7841; (*b*) S. C. Burdette, C. J. Frederickson, W. Bu and S. J. Lippard, *J. Am. Chem. Soc.*, 2003, **125**, 1778–1787; (*c*) E. M. Nolan, S. C. Burdette, J. H. Harvey, S. A. Hilderbrand and S. J. Lippard, *Inorg. Chem.*, 2004, **43**, 2624–2635; (*d*) C. J. Chang, E. M. Nolan, J. Jaworski, S. C. Burdette, M. Sheng and S. J. Lippard, *Chem. Biol.*, 2004, **11**, 203–210; (*e*) C. J. Chang, E. M. Nolan, J. Jaworski, K.-I. Okamoto, Y. Hayashi, M. Sheng and S. J. Lippard, *Inorg. Chem.*, 2004, **43**, 6774–6779; (*f*) C. C. Woodroofe, R. Masalha, K. R. Barnes, C. J. Frederickson and S. J. Lippard, *Chem. Biol.*, 2004, **11**, 1659–1666; (*g*) E. M. Nolan, J. Jaworski, K.-I. Okamoto, Y. Hayashi, M. Sheng and S. J. Lippard, *J. Am. Chem. Soc.*, 2005, **127**, 16812–16823; (*h*) G. K. Walkup, S. C. Burdette, S. J. Lippard and R. Y. Tsien, *J. Am. Chem. Soc.*, 2000, **122**, 5644–5645; (*i*) X. Zhang, K. S. Lovejoy, A. Jasanoff and S. J. Lippard, *Proc. Natl. Acad. Sci. U. S. A.*, 2007, **104**, 10780–10785; (*j*) B. A. Wong, S. Friedle and S. J. Lippard, *J. Am. Chem. Soc.*, 2009, **131**, 7142–7152; (*k*) X. Zhang, D. Hayes, S. J. Smith, S. Friedle and S. J. Lippard, *J. Am. Chem. Soc.*, 2008, **130**, 15788–15789; (*l*) E. Tomat, E. M. Nolan, J. Jaworski and S. J. Lippard, *J. Am. Chem. Soc.*, 2008, **130**, 15776–15777.

8 (*a*) Z.-X. Han, X.-B. Zhang, Z. Li, Y.-J. Gong, X.-Y. Wu, Z. Jin, C.-M. He, L.-X. Jian, J. Zhang, G.-L. Shen and R.-Q. Yu, *Anal. Chem.*, 2010, **82**, 3108–3113; (*b*) K. Hanaoka, K. Kikuchi, H. Kojima, Y. Urano and T. Nagano, *Angew. Chem., Int. Ed.*, 2003, **42**, 2996–2999; (*c*) K. Hanaoka, K. Kikuchi, H. Kojima, Y. Urano and T. Nagano, *J. Am. Chem. Soc.*, 2004, **126**, 12470–12476; (*d*) T. Hirano, K. Kikuchi, Y. Urano, T. Higuchi and T. Nagano, *J. Am. Chem. Soc.*, 2000, **122**, 12399–12400; (*e*) T. Hirano, K. Kikuchi, Y. Urano and T. Nagano, *J. Am. Chem. Soc.*, 2002, **124**, 6555–6562.

9 (*a*) D. Srikun, E. W. Miller, D. W. Domaille and C. J. Chang, *J. Am. Chem. Soc.*, 2008, **130**, 4596–4597; (*b*) K. Komatsu, Y. Urano, H. Kojima and T. Nagano, *J. Am. Chem. Soc.*, 2007, **129**, 13447–13454; (*c*) W. Lin, L. Long, B. Chen and W. Tan, *Chem.–Eur. J.*, 2009, **15**, 2305–2309; (*d*) F. Qian, C. Zhang, Y. Zhang, W. He, X. Gao, P. Hu and Z. Guo, *J. Am. Chem. Soc.*, 2009, **131**, 1460–1468.

10 (*a*) A. Caballero, R. Martinez, V. Lioveras, I. Ratera, J. Vidal-Gancedo, K. Wurst, A. Tarraga, P. Molina and J. Veciana, *J. Am. Chem. Soc.*, 2005, **127**, 15666–15667; (*b*) K. Kiyose, H. Kojima, Y. Urano and T. Nagano, *J. Am. Chem. Soc.*, 2006, **128**, 6548–6549; (*c*) Z. Xu, K.-H. Baek, H. N. Kim, J. Cui, X. Qian, D. R. Spring, I. Shin and J. Yoon, *J. Am. Chem. Soc.*, 2010, **132**, 601–610; (*d*) L. Xue, Q. Liu and H. Jiang, *Org. Lett.*, 2009, **11**, 3454–3457; (*e*) Z. Liu, C. Zhang, Y. Li, Z. Wu, F. Qian, X. Yang, W. He, X. Gao and Z. Guo, *Org. Lett.*, 2009, **11**, 795–798; (*f*) S. Maruyama, K. Kikuchi, T. Hirano, Y. Urano and T. Nagano, *J. Am. Chem. Soc.*, 2002, **124**, 10650–10651; (*g*) M. Taki, J. L. Wolford and T. V. O'Halloran, *J. Am. Chem. Soc.*, 2004, **126**, 712–713; (*h*) C. C. Woodroofe and S. J. Lippard, *J. Am. Chem. Soc.*, 2003, **125**, 11458–11459; (*i*) C. J. Chang, J. Jaworkski, E. M. Nolan, M. Sheng and S. J. Lippard, *Proc. Natl. Acad. Sci. U. S. A.*, 2004, **101**, 1129–1134; (*j*) L. Xue, C. Liu and H. Jiang, *Chem. Commun.*, 2009, 1061–1063.

11 (*a*) D. A. Pearce, N. Jotterand, I. S. Carrico and B. Imperiali, *J. Am. Chem. Soc.*, 2001, **123**, 5160–5161; (*b*) G. Xue, J. S. Bradshaw, N. K. Dalley, P. B. Savage, R. M. Izatt, L. Prodi, M. Montalti and N. Zaccheroni, *Tetrahedron*, 2002, **58**, 4809–4815; (*c*) Y. Mikata, M. Wakamatsu and S. Yano, *Dalton Trans.*, 2005, 545–550.

12 (*a*) S. Petruso and S. Caronna, *J. Heterocycl. Chem.*, 1992, **29**, 355–357; (*b*) S. Mula, A. K. Ray, M. Banerjee, T. Chaudhuri, K. Dasgupta and S. Chattopadhyay, *J. Org. Chem.*, 2008, **73**, 2146–2154.

13 L. Jiao, C. Yu, J. Li, Z. Wang, M. Wu and E. Hao, *J. Org. Chem.*, 2009, **74**, 7525–7528.

14 L. Xue, C. liu and H. Jiang, *Org. Lett.*, 2009, **11**, 1655–1658.

15 (*a*) H. Sunahara, Y. Urano, H. Kojima and T. Nagano, *J. Am. Chem. Soc.*, 2007, **129**, 5597–5604; (*b*) K. Rurack, M. Kollmannsberger, U. Resch-Genger and J. Daub, *J. Am. Chem. Soc.*, 2000, **122**, 968–969; (*c*) M. Kollmannsberger, K. Rurack, U. Resch-Genger and J. Daub, *J. Phys. Chem. A*, 1998, **102**, 10211–10220.

16 M. Frisch, G. Trucks, J. Cheeseman, G. Scalmani, F. Clemente, H. Hratchian, M. Caricato, A. Izmaylov, J. Hess, C. Adria, *et al. Gaussian 09, Revision A1[M]*, Wallingford CT: Gaussian Inc., 2009.

17 T. Cheng, T. Wang, W. Zhu, Y. Yang, B. Zeng, Y. Xu and X. Qian, *Chem. Commun.*, 2011, **47**, 3915–3917.

18 E. Kawabata, K. Kikuchi, Y. Urano, H. Kojima, A. Odani and T. Nagano, *J. Am. Chem. Soc.*, 2005, **127**, 818–819.

 This journal is © The Royal Society of Chemistry 2012